

Summary of Environmentally Induced Electrical Discharges on the P78-2 (SCATHA) Satellite

H.C. Koons*

The Aerospace Corporation, El Segundo, California

The mission of the P78-2 (SCATHA) satellite, launched in January 1979, is to measure parameters related to the spacecraft charging process near synchronous orbit. The pulse analyzer experiment onboard measures the shape of pulses on four sensors. To date, 447 days of data have been analyzed. Thirty-four pulses on twenty different days have been related to electrical discharges resulting from spacecraft charging. A variety of pulse shapes are observed with dominant frequencies between 5 and 32 MHz and peak amplitudes from 0.08 to 30.1 V into a 50- Ω load. The amplitude of four of the pulses exceeded by a factor of five those measured during systems level factory test. This indicates that the present test specification is inadequate to simulate the EMI levels experienced by a payload from worst-case on-orbit discharges.

Introduction

THE P78-2 (SCATHA) satellite was launched on January 30, 1979. The primary objective of the mission was to obtain environmental and engineering data that could be used to provide design guidelines and materials, process and test specifications to insure that future spacecraft will operate satisfactorily in a spacecraft charging environment. The experiments are described by Stevens and Vampola¹ and Fennell.²

The engineering payloads include a charging electric effects analyzer (CEEA) to measure the characteristics of electrical discharges in both the frequency and the time domain, and three satellite surface potential monitors (SSPMs) to measure surface potentials of typical spacecraft thermal control materials such as Kapton, quartz fabric, and optical solar reflectors. Another experiment, the Sheath Electric Fields Experiment (SEFE), uses ion and electron measurements to infer the electric field in the plasma sheath near the satellite and the potential of the satellite with respect to the space plasma. Electron and ion beam emission systems were also provided for charging and discharging the satellite.³

The results of the CEEA payload are summarized in this paper. The primary objective of this payload is to verify that electrical discharges are occurring when other instruments measure large differential potentials between surface materials on the vehicle.

The CEEA consists of three instruments: a pulse analyzer, a VLF analyzer, and an RF analyzer. The pulse analyzer measures the number of pulses, their amplitudes and shapes on four sensors. The VLF analyzer measures the electric and magnetic field spectra of waves in the frequency range from ~100 Hz to 300 kHz. The RF analyzer measures the electric field intensity on a 1.8-m monopole antenna in the frequency range from 2 to 30 MHz.

Pulses are detected in response to commands, during electron and ion beam experiments and during periods of natural charging. The pulse analyzer, which measures the shape of pulses on four sensors, is the primary CEEA diagnostic for the natural discharges. To date, 447 days of pulse analyzer data have been analyzed. Thirty-four pulses on twenty different days have been related to natural discharges.

Some of these are correlated with the solar illumination of the vehicle.

In this paper, results from the pulse analyzer from 447 days between 7 February 1979 and 23 April 1981 are presented. This period covers quiet and active days, eclipses, and electron and ion beam operations. The instrument is described in the next section, followed by a presentation of the pulse statistics. Individual time periods of special interest are described in detail. In the final sections the aspect dependence and frequency spectrum of the natural discharges are described, and the pulses detected on orbit are compared with those detected during systems-level factory tests.

Instrument Description

The pulse analyzer measures the shape of electromagnetic pulses in the time domain from 7 ns to 3.7 ms. The pulse analyses are made on four sensors: 1) a loop antenna around one of the two redundant space vehicle command distribution units; 2) a harness wire along the outside of a "typical" space vehicle cable bundle; 3) an external short dipole antenna at the end of a 2-m boom, and 4) a digital command line from the space vehicle command distribution unit to the pulse analyzer.

The instrument is commanded by a seven-bit serial magnitude command. The signal processor may be switched by command to any subset of the four sensors. It then steps automatically through the selected sensors monitoring each in turn for 16 s. The functional block diagram is shown in Fig. 1. When a signal exceeds a commandable threshold, its amplitude is sampled at 16 points to measure the pulse shape. The 16 samples may be spaced logarithmically or linearly in time. The logarithmic spacing covers the range from 7 ns to 492 μ s. The linear spacing is commandable with the following options: 0.015, 0.060, 0.24, 1.0, 3.8, 30, and 250 μ s. The amplitude is measured by a bank of 24 discriminators, 12 positive and 12 negative. The total range of the discriminator bank is 3 mV to 1.8 V. The signal from each sensor can be attenuated by command to place it within this range. There are six attenuation settings that select measurement ranges from 3 mV to 1.84 V at minimum attenuation to 3.46 to 1910 V at maximum attenuation. The threshold is coupled to the attenuation setting. The attenuation, threshold, and sampling interval can be independently commanded for each sensor. The number of pulses per second above four selectable thresholds is also measured. Three of the thresholds are determined by the attenuation selection, the fourth is the pulse analysis threshold. In-flight verification of the calibration of the instrument was accomplished by sending serial magnitude

Presented as Paper 82-0264 at the AIAA 20th Aerospace Sciences Meeting, Orlando, Fla., Jan. 11-14, 1982; submitted Jan. 22, 1982; revision received March 11, 1983. Copyright © American Institute of Aeronautics and Astronautics, Inc., 1982. All rights reserved.

*Senior Scientist, Space Sciences Laboratory.

commands on the digital command line from the space vehicle command distribution unit.

In its normal mode of operation the instrument steps through each of four sensors monitoring each for 16 s in sequence. The threshold and attenuations for each sensor were determined by experience on orbit. Initial measurements were made with the logarithmic sample spacing. Linear spacing (15 ns) has been used since October 1979 because typical pulses proved to be shorter than 200 ns.

Data

The pulse analyzer was turned on and successfully checked out on-orbit on February 5, 1979. Initial operations began with the pulse analysis threshold set at 0.65 V and the count-rate thresholds set as shown in column 1 of Table 1. At these settings only two pulses were detected during the 72 h of data available from February 12-14. Both of these pulses occurred during ion beam experiments on February 14. The pulses had a width at half maximum of 500 μ s and an amplitude of 0.7 V.

Because it was apparent that very few pulses were being detected, the threshold was lowered on February 18 to 0.165 V with the associated count-rate thresholds listed in column 2 of Table 1.

At this threshold the analyzer occasionally responds to pulses generated when commands are sent to the vehicle. Pulses occurring within 1 s of a command are attributed to a vehicle or payload response to the command and are identified in Table 2 as command pulse. An interesting variation to this is a pulse that occurs approximately 20 s after the vehicle transmitter is turned off. These have been identified with the time that the ground station command transmitter ceases sending s-tones to the vehicle (s-tones enable the space vehicle command receiver). They are identified as s-tone cessation pulses in Table 2.

A second source of pulses is the antenna switch in the VLF analyzer. This experiment is housed in the same package as the pulse analyzer. When the VLF antenna switches from a magnetic antenna to an electric antenna, a pulse is detected

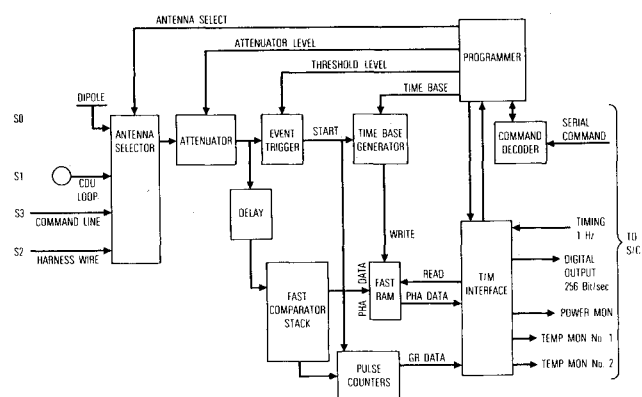


Fig. 1 Simplified block diagram of pulse analyzer.

on the pulse analyzer command line sensor. This pulse occurs once every 64 s. Since these pulses are synchronized to the vehicle clock they can be readily identified and have been eliminated from the distributions in Table 2.

The majority of the remaining pulses listed in Table 2 occurred during the electron and ion beam experiments.

Natural Charging

Only 34 of the 4640 pulses cannot be associated with normal vehicle commands or ion and electron beam operations. A summary of these pulses is shown in Table 3. Many of these pulses occurred during periods of natural charging. Pulses that occurred when the surface of the satellite was charged are identified in Table 3 by large voltages between the Kapton samples on the SSPMs and the satellite frame.

On March 28, surface charging occurred while the vehicle was eclipsed by the shadow of the Earth. This day was unusual in that the satellite was in the Earth's shadow over 1000 s before an injection of hot plasma near local midnight charged the vehicle negatively. Figure 2 shows a composite of data from the satellite surface potential monitor (SSPM), the pulse analyzer, and the electron and ion detectors on the Sheath Electric Fields Experiment (SEFE). The differential potential between a Kapton sample and the vehicle frame is plotted as a function of time in the bottom panel. At the time the Kapton potential abruptly increases from background to over 1 kV, the mean electron energy increases from about 1 kV to greater than 20 kV. About 5 min later a discharge was detected by the pulse analyzer. Later, a second discharge and a decrease in the average Kapton potential occurred as the satellite crossed the terminator from shadow into sunlight. During this charging event, the vehicle frame increased to ~8000 V and maintained a potential near -4000 V until the

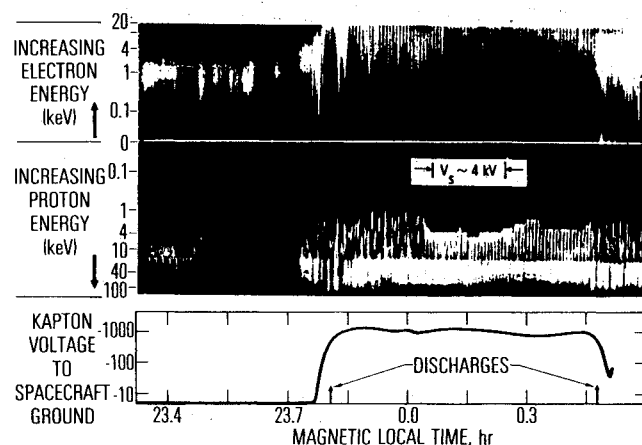


Fig. 2 Electron and proton energy fluxes and Kapton voltage with respect to the vehicle structure during a spacecraft charging event on March 28, 1979 in the Earth's eclipse. In the two top panels a brighter image represents greater particle fluxes.

Table 1 Pulse analyzer settings

	Time period				
	2/05/79 to 2/17/79	2/18/79 to 4/26/79	4/27/79 to 10/11/79	10/11/79 to 3/24/80	3/14/80 to 4/23/81
Thresholds, V					
Pulse analysis	0.651	0.165	0.327	0.327	0.165
Count rate CR0	0.117	0.030	0.117	0.117	0.030
Count rate CR1	1.85	0.469	1.85	1.85	0.469
Count rate CR2	28.3	7.18	28.3	28.3	7.18
Count rate CR3	0.651	0.165	0.327	0.327	0.165
Pulse analysis range	0.05-29.2	0.014-7.43	0.05-29.2	0.05-29.2	0.014-7.43
Time state	log	log	log	linear (15 ns)	linear (15 ns)

Table 2 Distribution of pulses detected by the pulse analyzer in 447 days of analyzed data

Command pulses	2287
s-Tone cessation	905
Electron beam	1099
Ion beam	315
Discharges	34
Total	4640

Table 3 Summary of discharges

Date	UT, s	LT, h	Radius, R_e	Kapton, V	Comment
3/28/79	59,851	23.8	6.3	-1725	Electron injection
3/28/79	62,088	0.4	6.5	-1689	Umbral exit + 50 s
4/14/79	39,940	0.2	6.7	-400	Eclipse
4/18/79	82,767	10.8	6.3	None	
4/30/79	25,616	1.2	7.4	-840	One sample $\neq 0$
5/26/79	2,641	2.6	7.8	-1098	Same spin phase
5/26/79	2,756	2.7	7.8	-1049	Same spin phase
5/26/79	2,928	2.7	7.8	-1074	Same spin phase
5/26/79	3,158	2.7	7.8	-1061	Same spin phase
5/26/79	3,387	2.8	7.8	-1012	Same spin phase
5/26/79	3,444	2.8	7.8	-1061	Same spin phase
9/09/79	2,095	2.3	6.7	-200	
9/18/79	35,981	1.5	6.2	-300	
1/24/80	3,082	12.3	5.4	None	
4/16/80	22,281	0.5	7.2		Umbral exit + 92 s
6/13/80	4,322	14.0	5.3	None	
6/13/80	6,750	15.0	5.6	None	
6/14/80	5,400	15.0	5.4	None	
6/14/80	9,770	16.7	5.6	None	
6/20/80	20,132	21.6	7.2		
3/09/81	920	6.8	7.7		
3/13/81	53,258	23.8	5.8	-1000	Umbral
3/13/81	53,262	23.8	5.8	-1000	Umbral
3/13/81	53,263	23.8	5.8	-1000	Umbral
3/21/81	6,318	10.8	7.1		
3/30/81	46,222	3.5	7.2		
3/31/81	35,005	1.1	6.5		
4/01/81	34,568	1.3	6.5	-1500	
4/01/81	34,920	1.3	6.5	-1500	
4/01/81	35,215	1.4	6.6	-1500	
4/23/81	3,023	0.0	6.5	-883	
4/23/81	4,016	0.1	6.6	-308	
4/23/81	4,150	0.1	6.6	-655	
10/8/81	72,375	23.9	6.5		Umbral

spacecraft entered sunlight. The data in Fig. 2 confirm that the spacecraft charging induced by energetic electrons produced significant differential potentials and electrical discharges. The low energy limit of the protons in Fig. 2 represents the potential of the spacecraft frame relative to the plasma environment. This is seen to fluctuate around ~ -4 kV during the charging event. The potential between the Kapton sample and the plasma is found by adding the -4 kV of the spacecraft frame to the Kapton voltage.

On May 26, 1979 a series of six pulses was detected by the pulse analyzer while the vehicle was in sunlight. These pulses occurred during the enhancement of the differential potential of a Kapton sample on the SSPM on the end of the vehicle (Fig. 3). At that time the spin axis of the vehicle made an angle of 90 deg with the sun-satellite line. At that angle this Kapton sample was shadowed by the vehicle and could not be discharged by sunlight.

The highest charging levels and largest discharges detected by SCATHA occurred on April 23, 1981. During the spring of 1981, eclipse season for geostationary satellites, the occurrence and magnitudes of magnetic storms increased. Magnetic indices show that April 1981 had some of the most disturbed days during the current sunspot cycle.

Figure 4a shows the P78-2 spacecraft frame potential during the charging period on April 23, 1981. The potential

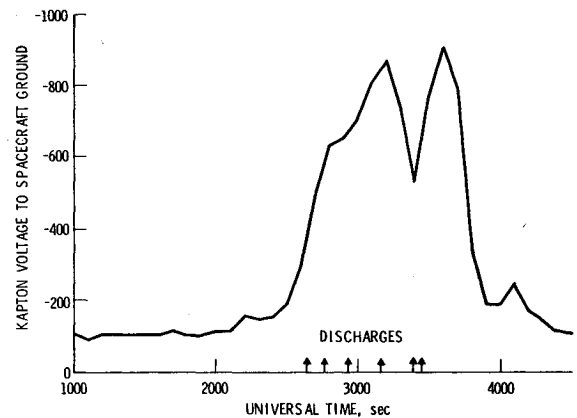


Fig. 3 Kapton voltage with respect to the vehicle structure during a spacecraft charging event on May 26, 1979. The arrows identify the times of six discharges detected during this period.

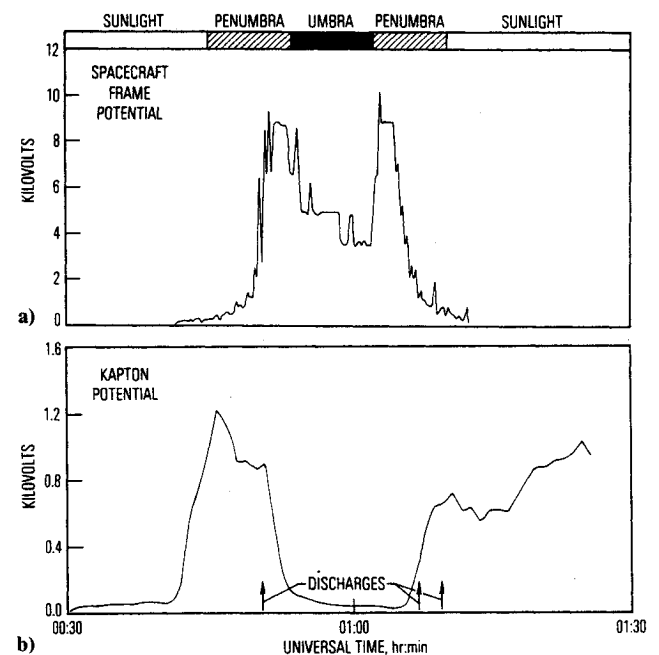


Fig. 4 Spacecraft frame potential a) and Kapton voltage with respect to the vehicle structure b) during a spacecraft charging event on April 23, 1981. The arrows identify the times of three discharges detected during this period.

was determined from charged-particle distributions measured by the SEFE instrument. For each satellite rotation of 1-min duration, four estimates of the vehicle potential were made from shifts in the energy of the ion spectrum. The vehicle began to charge negatively near 00:42 UT, just prior to entering the Earth's penumbra. Before entering the umbra near 00:55 UT, the potential of the satellite frame reached nearly -9000 V. During passage through the umbra, the potential dropped below 4000 V and then increased to $\approx -10,000$ V when the Earth's penumbra was again encountered near 01:03 UT. By the time the spacecraft entered full sunlight near 01:10 UT, the vehicle frame had dropped to a few hundred volts negative potential.

Figure 4b shows the differential voltage between one of the Kapton samples on the SSPM experiment and the vehicle frame. This Kapton sample is on the SSPM instrument on the top of the spacecraft. At this time this instrument was in the shadow of the vehicle and the Kapton could not be discharged by the solar ultraviolet light. With the vehicle in full sunlight, both the Kapton sample and the vehicle frame potential began to charge significantly near 00:42 UT. The maximum

potential for Kapton was reached near 00:46 UT with a value very close to -1200 V. As the vehicle entered the penumbra near 00:46 UT, the frame potential continued to charge negative and the potential of the Kapton with respect to this reference reached its maximum differential potential of approximately -1200 V.

The arrows along the time axis in Fig. 4 indicate when discharge pulses were detected by the pulse analyzer. The first discharge pulse at 00:50:23 UT occurred when the Kapton dielectric surface potential was dropping with respect to the spacecraft frame. The change in the relative potential between a shadowed dielectric and spacecraft ground occurs because the vehicle frame rapidly charges negatively. The discharge occurred when a large change occurred in the frame potential. The Kapton surface was already charged negatively to approximately -900 V prior to the time of the discharge. Following the discharge, as the solar ultraviolet (UV) flux which illuminates the vehicle decreased, the satellite frame charged to almost -9000 V. Subsequently, the Kapton potential with respect to the vehicle frame dropped to less than -1000 V. The second and third discharge pulses were recorded at 01:06:56 and 01:09:10 UT. By this time the vehicle frame potential had decreased due to increased solar UV flux and the dielectric surface potentials were becoming more negative relative to satellite frame potential. All three discharges occurred during periods when the differential potentials were undergoing large changes.

Most of the remaining pulses also occurred during time periods when the Kapton samples on the satellite surface potential monitors were charged. The amplitude distribution of the discharges is shown in Fig. 5b. The location of the satellite at the time these pulses occurred is shown in Fig. 6 as a function of local time and radial distance. This distribution

is consistent with the local time dependence of circuit upsets on Department of Defense (DoD) and commercial satellites.⁴

The data plotted at afternoon local times in Fig. 6 demonstrate that discharges can also occur on the day side of the Earth following moderate magnetic storms. Four of these pulses occurred on June 13 and June 14, 1980 at altitudes well below geosynchronous altitude. The Boulder Geomagnetic Substorm Log lists a moderate substorm at 07:45 UT on June 11, with a second onset at 22:30 UT on June 11, followed by minor magnetic storm conditions throughout the day on June 12 and 13. Since the vehicle was not charged at the time these discharges were detected, it is likely that they were due to cable breakdowns. These occur when energetic electrons in the outer radiation belt penetrate and charge the dielectrics in coaxial cables. The flux of energetic electrons is enhanced following a magnetic storm. During this June 1980 time period, P78-2 experienced the largest fluxes of energetic (>300 keV) electrons since launch.⁵

Aspect Dependence

The six discharges detected on May 26 occurred at the same rotational phase of the vehicle. Since the vehicle was in sunlight, this suggests that one location on the vehicle was arcing. Presumably this would occur when the potential difference suddenly increased as material on one side of the arc was discharged by photocurrent as it passed into sunlight.

Table 4 Solar direction in satellite coordinates at time of pulse

Date	UT, s	Elevation, deg	Azimuth, ^a deg
3/28/79	59,851	90.7	19.4
3/28/79	62,088	90.7	12.6
4/14/79	39,940	84.7	91.5
4/18/79	82,767	88.7	307.9
4/30/79	25,616	87.2	287.2
5/26/79	02,641	90.3	265.4
5/26/79	02,756	90.3	263.8
5/26/79	02,928	90.3	264.5
5/26/79	03,158	90.3	261.3
5/26/79	03,387	90.3	264.3
5/26/79	03,444	90.3	266.6
8/9/79	02,095	86.0	51.5

^a Measured counterclockwise from $+z$ axis in spacecraft coordinate system.

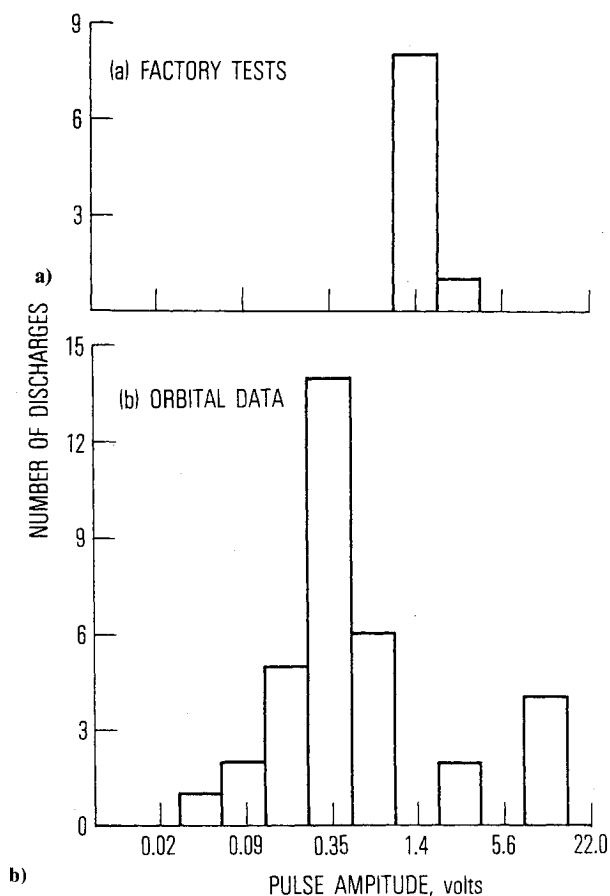


Fig. 5 Histograms of pulse amplitude distribution. a) Pulses measured during preflight, factory, electrical-discharge tests. b) Discharges measured on orbit.

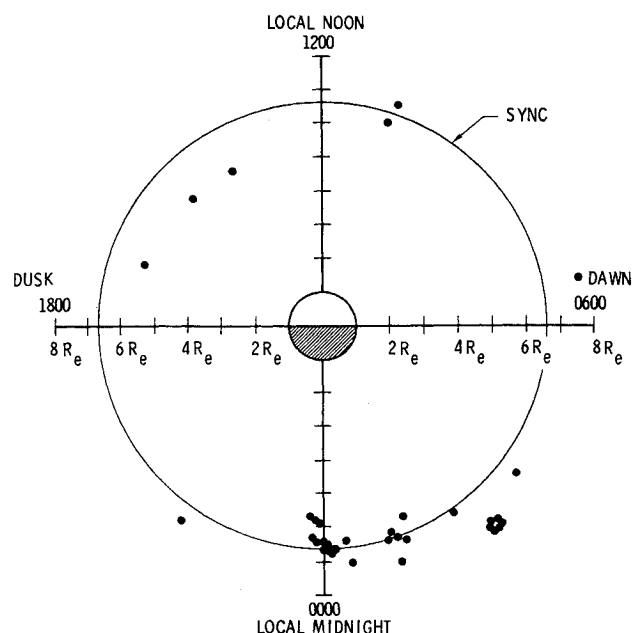


Fig. 6 Satellite location in radial distance and local time when discharges were detected.

Table 5 Natural discharge fitting parameters

Date	UT, s	Sensor	<i>i</i>	Frequency, <i>f</i> , MHz	Amplitude, <i>v_i</i> , V	Damping, <i>k_i</i> , 1/ns	Phase angle, <i>φ_i</i> , deg
4/23/81	3023	CDU loop	0	0.06			
			1	6.2	1.69	0.0077	32
			2	17.8	1.69	0.0087	58
			3	29.5	2.2	0.005	153
4/23/81	4016	Harness wire	0		0.18		
			Exp		15.8	0.027	
			1	11.8	30.1	0.022	-89
			2	20.7	2.6	-0.00097	226
4/23/81	4150	Dipole	3	29.7	19.0	0.0077	-27
			0		0.49		
			1	5.4	11.3	0.14	58
			2	18.0	16.8	0.0204	215
			3	26.3	9.1	0.1	20

Table 6 Pulse fitting parameters

Date	UT, s	Sensor	i	f_i , MHz	u_i , V	k_i, k_i , 1/ns	ϕ_i, ϕ_i , deg
Electron gun pulse							
3/23/80	51096	CMD line	0		-0.003		
			1	14.1	0.089	$+3.57 \times 10^{-3}$	182.4
			2	26.4	0.140	-1.32×10^{-3}	46.9
VLF antenna pulse							
3/23/80	51860	CMD line	0		-0.007		
			1	9.0	0.397	3.67×10^{-2}	45.6
			2	16.0	0.135	3.95×10^{-3}	227.3

In order to determine if discharges on other dates occurred at the same rotational phase, the azimuth and elevation of the sun in spacecraft coordinates was calculated for a number of other discharges. The results are tabulated in Table 4. There is a large scatter in the data implying that the location and mechanism described above for the May 26 discharges are not the same for the others. The sun does tend to be 180 deg from the magnetometer boom suggesting that this boom plays a role in a significant number of the discharges. NASCAP computer results for models of the SCATHA satellite show the largest differential potentials occur at the booms.⁶

Frequency Spectrum

Twenty discharge pulses have been detected with the pulse analyzer in a mode of operation with a linear sample spacing of 15 ns. These data have been used to determine the dominant frequency components in each pulse. A computer fit of the functional form

$$V = V_0 + \sum V_i e^{-k_i t} \cos(2\pi f_i t + \phi_i)$$

was made to the sixteen sample points measured for each pulse. For highly damped waveforms, a decaying exponential term was also included in the sum. The twenty discharge pulses are quite different with dominant frequencies from 5 to 32 MHz and peak amplitudes from 0.08 to 30.1 V.

Table 5 lists the discharge fitting parameters used to characterize the three pulses measured by the pulse analyzer that resulted from the differential charging on April 23, 1981. Figure 7 shows the corresponding fits to these pulses. A second pulse detector, the transient pulse monitor,² measured the amplitude of these pulses to be 44, 13, and 108 V into a 10-kΩ impedance. Two of the three pulses on April 23, 1981 were the largest pulses detected on SCATHA in 27 months of operation.

To date too few natural discharge pulses have been found to adequately characterize the discharges for the purpose of

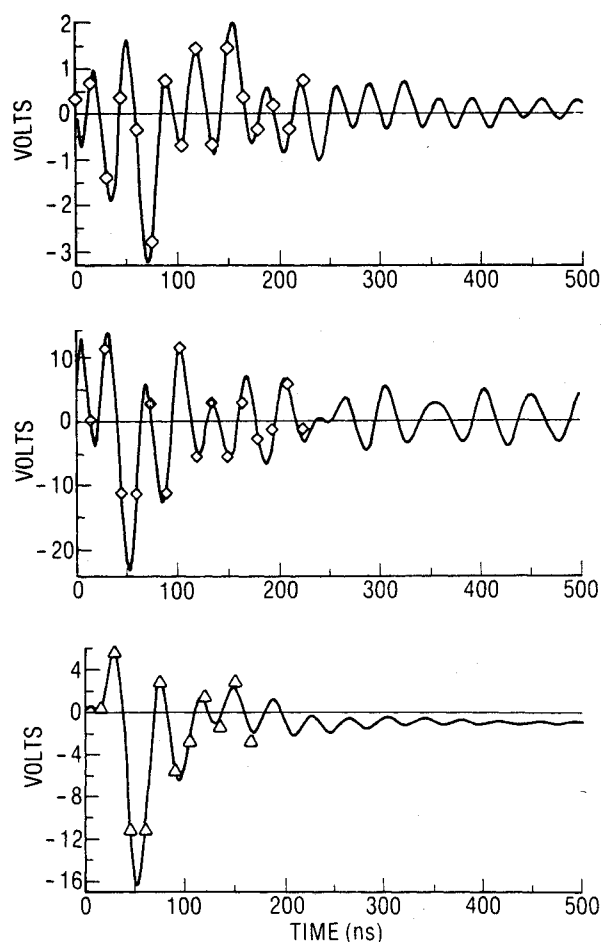


Fig. 7 Pulse shapes for the three large discharges observed on April 23, 1981.

validating discharge coupling models and ground-based discharge tests using scale-sized models of the SCATHA satellite.

Electron Beam Experiments

Pulses are also detected during electron and ion beam experiments. During the electron beam experiments on March 30, 1979, two plasma potential sensors failed. These sensors were part of the Sheath Electric Fields Experiment. Data obtained from the pulse analyzer and the RF analyzer show that discharges were occurring on the vehicle at the time of the failure. Two of the largest pulses occurred at the times the sensors failed.

Pulses exceeding the 0.165-V analysis threshold abruptly onset at 15:12:08 UT at the time the electron beam was commanded to a -3 kV potential at 6 mA current. Pulses above threshold continued until 15:51:24 UT. Pulses of comparable magnitude occurred on each of the four pulse analyzer sensors. The largest count rate threshold was 7.18 V. The number of pulses above this threshold is shown in Fig. 8 as a function of time. Only once did two pulses occur in 1 s. Since the highest discriminator level was exceeded by about 10% of the pulses, the thresholds were reset to the value shown in column 3 of Table 1, on April 27, 1979. At the time these pulses occurred, the RF analyzer was operating on the 1.8-m monopole antenna at fixed frequency of 20 MHz with a bandwidth of 4 kHz. The data from the RF analyzer are shown in Fig. 9. The pulses began at 15:12:08 UT. The plasma potential sensors failed during two of the larger pulses detected by the RF analyzer. The peak power of -83 dBm in a 4 kHz bandwidth at 20 MHz cannot be considered very large at that frequency.

The VLF analyzer also shows pulses during the electron beam experiments. Broadband VLF data are available from the beam experiments on April 24, 1979. The VLF analyzer detects many low-level pulses that do not exceed the pulse analyzer threshold.

On March 23, 1980, the pulse analyzer detected a pulse at 1411:36 UT during electron beam operations at 1.5 kV 1 mA. At 1424:20 UT a pulse due to the automatic antenna switch in the VLF experiment was detected. Both pulses were measured on the command sensor line in the high resolution mode. A computer fit was made to the pulse shapes of these pulses in order to compare them with the discharge-related pulses. The parameters giving the best fit are shown in Table 6. For the pulse during electron beam operations, that best fit was obtained for two frequencies. One of the two frequencies showed a slight growth rate while the other was slightly damped. The pulse shape is shown in Fig. 10. The damping is probably very small and the data set too short to determine the damping coefficient. For the antenna switch pulse the best fit was again obtained from two frequencies. The frequencies differ significantly from those obtained for the electron beam pulse. The antenna switch pulse is also shown in Fig. 10.

Ion Gun Experiments

On Feb, 14, April 5, and April 24, 1979 pulses were detected by the pulse analyzer during an ion beam-induced charging event. Impulses appeared across the VLF spectrum essentially continuously after the ion beam was turned on. Few of these low-level pulses were detected by the pulse analyzer.

Comparison of Flight Data with Prelaunch Test Data

The SCATHA satellite underwent a series of arc injection tests at the systems level during factory testing. The tests were conducted according to the electrostatic discharge specification in MIL-STD-1541. A total of 11 arcs at 20 kV were discharged to various locations on the vehicle.

During these arc injection tests the harness wire sensor was monitored by the pulse analyzer. The threshold was set at 1.27 V and the logarithmic time spacing was used. The pulse analyzer detected 9 of the 11 arcs. The test arcs produced 1- to 2-V signals in the harness wire sensor. Only two arcs to the solar array produced signals that lasted longer than a few tens of nanoseconds. The amplitude distribution of these nine arcs is shown in Fig. 5a. Because the instrument was in the logarithmic time spacing mode it was not possible to obtain a pulse shape. It is unfortunate that a lower attenuation and threshold was not chosen for these tests. However, the data were not available for processing before the vehicle configuration was changed for other scheduled tests. Expecting much larger signals, most of the samples turned out to be zero.

The purpose of the MIL-STD-1541 electrostatic discharge test is to subject the space vehicle systems to pulses at least 6

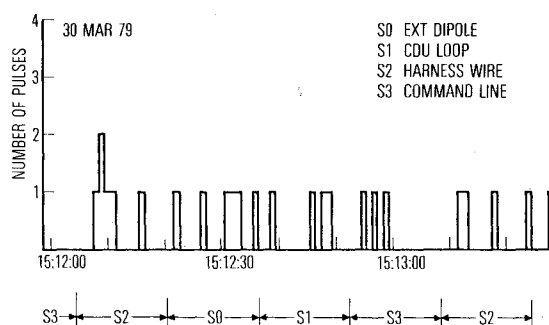


Fig. 8 Number of pulses exceeding a threshold of 7.18 V as a function of time during electron beam operations on March 30, 1979.

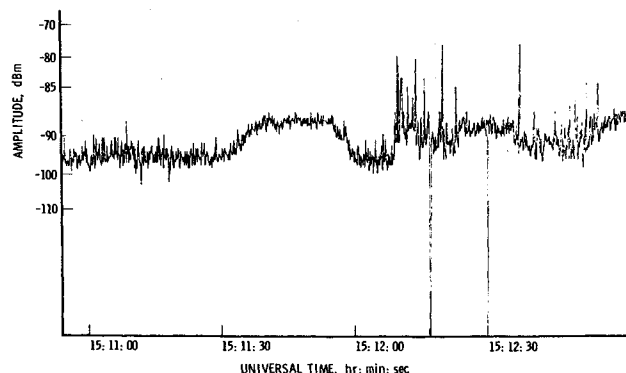


Fig. 9 Amplitude of the signal detected on the 1.8-m monopole antenna by RF analyzer on March 30, 1979 as a function of time.

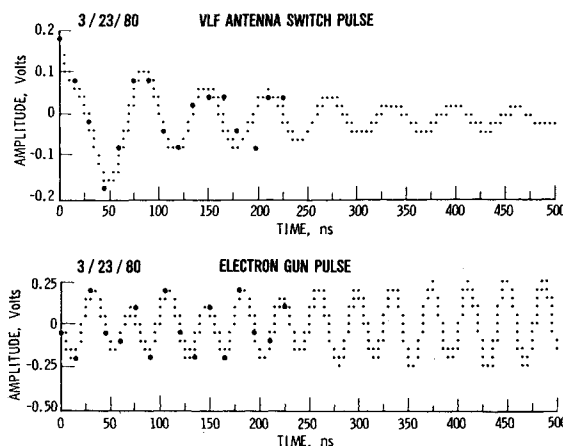


Fig. 10 Pulse shapes measured in the high resolution mode. The heavy dots are the measured points.

dB above the level to be expected on orbit. If each payload survives this test, it should survive discharges during spacecraft charging periods on orbit.

Figure 5 also shows the amplitude distribution of the 34 discharges detected on orbit. By comparing the distribution in Fig. 5b with the distribution in Fig. 5a, it can be seen that the MIL-STD-1541 electrostatic discharge test was an adequate test for all but the four largest pulses that occurred in April 1981. However, signals from the four largest pulses exceeded signals from the test pulses by about a factor of five. Therefore, the current MIL-STD test is inadequate to simulate worst-case on-orbit discharges.

Summary and Conclusions

The pulse analyzer onboard the P78-2 (SCATHA) satellite detects pulses during some time periods when the satellite surface potential monitors measure significant (>1000 V) potentials between selected sample materials and the spacecraft frame (ground). These pulses are likely to be electrical discharges resulting from differential potentials set up by spacecraft charging by energetic electrons. Thirty-four pulses on twenty different days have been identified as electrical discharges.

The amplitude of four of the pulses exceeded the amplitude of pulses measured during factory systems tests. The factory tests were conducted according to the MIL-STD-1541 electrical discharge test specification. The fact that the instrument

experienced larger pulses on orbit than it did during the factory tests demonstrates the inadequacy of the factory test to simulate the pulse amplitudes experienced by a satellite payload from worst-case on-orbit discharges.

Acknowledgment

This work was supported by the U.S. Air Force, Space Division under Contract No. F04701-82-C-0083.

References

- ¹Stevens, J.R. and Vampola, A.L., "Description of the Space Test Program P78-2 Spacecraft and Payloads," SAMSO TR-78-24, The Aerospace Corporation, Oct. 1978.
- ²Fennell, J.F., "Description of P78-2 (SCATHA) Satellite and Experiments, in *The IMS Source Book*, edited by Russell and Southwood, American Geophysical Union, Washington, D.C., 1982.
- ³Cohen, H.A., "P78-2 Satellite and Payload Responses to Electron Beam Operations on 30 March 1979," *Spacecraft Charging Technology 1980*, edited by N.J. Stevens and C.P. Pike, NASA Conference Publication 2182, NASA Science and Technical Information Office, 1981.
- ⁴McPherson, D.A., Cauffman, D.P., and Schober, W.R., "Spacecraft Charging at High Altitudes: SCATHA Satellite Program," *Journal of Spacecraft and Rockets*, Vol. 12, Oct. 1975, pp 621-626.
- ⁵Reagan, J., private communication, Lockheed Palo Alto, Oct. 1980.
- ⁶Stevens, N.J., private communication, NASA Lewis Research Center, Oct. 1980.

From the AIAA Progress in Astronautics and Aeronautics Series . . .

AEROTHERMODYNAMICS AND PLANETARY ENTRY—v. 77 HEAT TRANSFER AND THERMAL CONTROL—v. 78

Edited by A. L. Crosbie, University of Missouri-Rolla

The success of a flight into space rests on the success of the vehicle designer in maintaining a proper degree of thermal balance within the vehicle or thermal protection of the outer structure of the vehicle, as it encounters various remote and hostile environments. This thermal requirement applies to Earth-satellites, planetary spacecraft, entry vehicles, rocket nose cones, and in a very spectacular way, to the U.S. Space Shuttle, with its thermal protection system of tens of thousands of tiles fastened to its vulnerable external surfaces. Although the relevant technology might simply be called heat-transfer engineering, the advanced (and still advancing) character of the problems that have to be solved and the consequent need to resort to basic physics and basic fluid mechanics have prompted the practitioners of the field to call it thermophysics. It is the expectation of the editors and the authors of these volumes that the various sections therefore will be of interest to physicists, materials specialists, fluid dynamicists, and spacecraft engineers, as well as to heat-transfer engineers. Volume 77 is devoted to three main topics, Aerothermodynamics, Thermal Protection, and Planetary Entry. Volume 78 is devoted to Radiation Heat Transfer, Conduction Heat Transfer, Heat Pipes, and Thermal Control. In a broad sense, the former volume deals with the external situation between the spacecraft and its environment, whereas the latter volume deals mainly with the thermal processes occurring within the spacecraft that affect its temperature distribution. Both volumes bring forth new information and new theoretical treatments not previously published in book or journal literature.

Volume 77—444 pp., 6 × 9, illus., \$30.00 Mem., \$45.00 List
Volume 78—538 pp., 6 × 9, illus., \$30.00 Mem., \$45.00 List

TO ORDER WRITE: Publications Order Dept., AIAA, 1633 Broadway, New York, N.Y. 10019